Linking Chemical Transformations of Silver and Silver Nanoparticles in the Extracellular and Intracellular Environment to their Bio-reactivity.

Matteo Minghetti,[a] William Dudefoi,[a] Qing Ma,[b] and Jeffrey G. Catalano[c]

[a.] Department of Integrative Biology, Oklahoma State University, Stillwater, OK, USA.

[b.] DND-CAT, Northwestern Synchrotron Research Center at Advanced Photon Source, Argonne, IL, USA.

[c.] Department of Earth and Planetary Sciences, Washington University, Saint Louis, MO, USA.

Corresponding author

Address: Department of Integrative Biology, 501 Life Sciences West, Oklahoma State University, Stillwater, OK 74078.

Email: matteo.minghetti@okstate.edu

Abstract

The fish intestine is an important barrier for environmental toxicants, including metals and metal nanoparticles. Tracking chemical transformation at the interface between the intestinal epithelium and the intestinal lumen can inform us about chemicals' bio-reactivity and toxicity but is challenging due to the lack of appropriate models. To allow for such investigations, a model of the fish intestine derived from rainbow trout (*Oncorhynchus mykiss*), the RTgutGC cell line, was used. Cells were exposed to silver nitrate ($AgNO_3$) or citrated coated silver nanoparticles (cit-AgNP) in Leibovitz's L-15 medium without amino acids and vitamins (L-15/ex), which allowed the determination of the extracellular silver species using a chemical equilibrium model. X-ray absorption spectroscopy (XAS) was used to track the intracellular silver speciation. Cellular toxicity, silver accumulation, and metallothionein (MT) mRNA levels were also measured. Cells accumulated the same concentrations of silver when exposed to equimolar amounts (i.e. 1, 5 and 10 μM) of $AgNO_3$ or cit-AgNP. However, $AgNO_3$ was shown to be more toxic than cit-AgNP. Intracellular silver speciation changed over time in both exposure series. After 1-hour, intracellular silver speciation was dominated by chloride complexation in both exposures. After 24 and 72 hours of exposure to cit-AgNP, ~ 7% of silver were complexed to cysteine whereas the remaining silver was AgNP. In cells exposed to $AgNO_3$ for 72 hours, 97% Ag was complexed to cysteine. A significant increase, compared to controls, in metallothionein mRNA levels at 24 and 72 hours of exposure to $AgNO_3$ and cit-AgNP can explain the formation of Ag-cysteine complexes. In sum, these data show that silver chloride species are bioavailable and that complexation to cysteine scavenges intracellular dissolved silver ions thus preventing toxicity. Silver nanoparticles present a similar but attenuated toxic response to $AgNO_3$. Thus, at least in acute exposures, existing risk assessment for dissolved silver species could be protective for nanosilver.

Keywords: silver nanoparticles, X-ray absorption spectroscopy, RTgutGC, silver speciation

Environmental Significance Statement

The antimicrobial properties of silver nanoparticles are being exploited in numerous applications, including food supplements and disease control in aquaculture, which may result in their dietary uptake by aquatic organisms. Our knowledge of the precise mechanism of uptake of silver and nano silver via the dietary route at the intestine is limited due to lack of an appropriate model to study interactions at the cell/medium interface. For instance, the bioavailability and toxicity of chloride complexes, which might form readily after silver nanoparticles intestinal dissolution, is poorly understood. By determining the relationship between extracellular and intracellular metal speciation, we can evaluate the bioavailability and toxicity of specific metal species. This information may prove instrumental in implementing new models for nanoparticles environmental risk assessment.

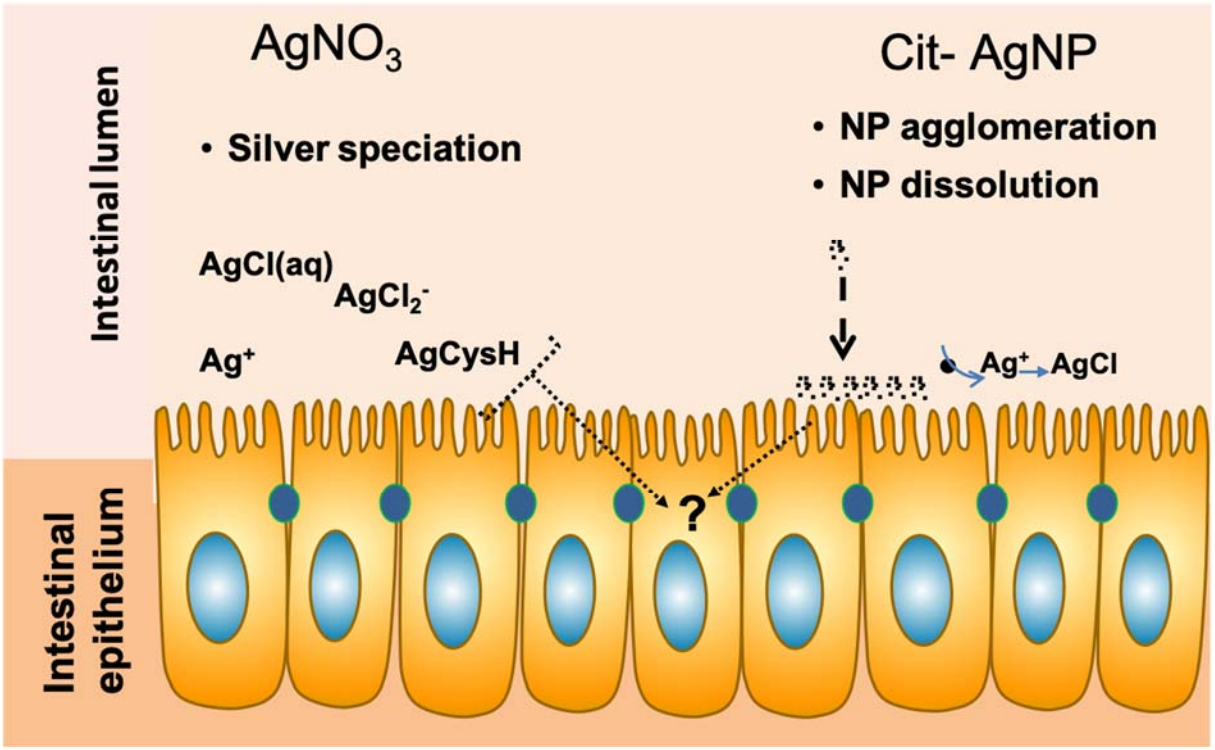

1. Introduction

Silver nanoparticles (AgNP) are clusters of silver atoms ranging from 1 to 100 nm in all three external dimensions[1] which, due to their increased antimicrobial properties, are used in a plethora of applications such as food additives, food packaging materials and water disinfectants[2]. Silver nanoparticles have also been proposed as effective alternatives to antibiotics for human and veterinary medicine[3,4], and, more recently, the use for disease control in aquaculture has been suggested[5]. The use of AgNP in these applications may result in the absorption of this material via the intestinal route both in humans and fish as environmental species. Despite the advantages that this technology brings about, their impact on human and environmental health is of concern[2] especially considering that absorptive processes at the intestine are currently poorly understood.

In order to understand the physiological role and toxicology of metals in dissolved or in colloidal form in the natural environment, one needs to be aware of the speciation of metals in abiotic and biotic compartments. The chemical species in which a metal is present in the extracellular environment (i.e., at the interface with the absorptive epithelium) determines its binding potential to biological ligands including glycoproteins present in the mucus and membrane proteins, which might reduce or enhance the uptake into the cell. Several studies have shown that the environmental (i.e., in the water column) free metal ion concentration can be a better predictor of metal toxicity in aquatic organisms than the total dissolved concentration[6]. However, metal speciation can vary significantly while transitioning from the water column to the extracellular environment. For instance, in fresh water, chloride concentration might be low (~0.03 to ~5 mM) while at the absorptive epithelium of the fish intestine it might be much higher (~70 to 150 mM)[7] resulting in the formation of different metal species[8]. Phenomena like competition with cations, complexation with anions and dissolved

organic matter influence the binding capacity of metals to “biotic” ligands, which is directly linked to their toxicity. These concepts are at the base of the biotic ligand model (BLM)[6], which is currently used by the U.S. Environmental Protection Agency and is being considered for use by the EU Water Framework Directive, as a tool to examine the toxicity of metals in the aquatic environment. However, there is emerging evidence that neutral[9], negatively, and positively charged metal complexes can be bioavailable and toxic[10,11] thus suggesting that the BLM might oversimplify the complex dynamics of metal uptake.

While uptake and homeostasis of dissolved metal ions - essential and non-essential - is tightly regulated by metal transporters[12–14] (Wang ACS nano), metal nanoparticles (MeNP) seem to bypass such mechanisms and enter the cell via endocytosis[11,15]. Therefore, MeNP uptake might be more difficult to control by the cell, resulting in the entry of a ‘big’ cargo of zero-valent MeNP into cellular vesicles. Depending on the vesicle’s internal milieu and MeNP solubility, metal ions will dissolve and possibly be transported out into the cytoplasm via metal transporters (Behra et al 2013) leaving the nano-material behind. The dissolved metal ion will then form different chemical species that will determine metal reactivity with cellular components, thus metal bio-reactivity and toxicity. For instance, certain NPs, such as AgNP, seem to be directed to lysosomes whose internal milieu is characterized by an acidic pH that likely induces dissolution of silver from the NP surface[11]. In addition, while commercial products might contain pristine AgNP, in natural water chemical transformations such as sulfidation have been shown to have an important role in determining toxicity of silver nanoparticles (AgNP) to aquatic organisms[16]. The decrease in AgNP toxicity appears to be related to the complexation with HS^-. Moreover, while fish exposure to pristine AgNP could be relevant in aquaculture, where pristine AgNP use has been proposed to improve water quality and for disease control[5], AgNP may also readily associate with environmental ligands (e.g. nutrients and other natural colloids). Therefore, determination of chemical transformations of metal NPs in the exposure medium (i.e., complexation of the metal ions dissolving from the NPs surface) is necessary to

understand their bioavailability and toxicity. While these considerations have been shown to be extremely useful in predicting toxicity of waterborne AgNP to fish embryos[17,18], they might not apply to dietary exposures. Indeed, we know very little about the chemical transformations that might occur in the intestinal lumen of fish - partially due to the lack of appropriate models to study such phenomena. Indeed, a better understanding of chemical transformations in the intracellular environment is necessary to predict nanoparticle bio-reactivity and toxicity.

To allow for such investigations at the NP/cell interface, we used a model of the fish intestine derived from Rainbow Trout (*Oncorhynchus mykiss*), the RTgutGC cell line[19]. RTgutGC is a unique intestinal fish cell line, which, when grown on permeable supports (transwells), forms a cell monolayer dividing the system into an upper (apical) and a lower (basolateral) compartment, thereby mimicking the intestinal lumen and the portal blood, respectively (Figure 1). RTgutGC cells grown on transwells develop a polarized epithelium characterized by expression of tight junction (ZO-1) and Na/K-ATPase proteins at the apical and basolateral membrane respectively[19]. Most importantly, RTgutGC cells tolerate exposures to well-defined synthetic simplified media that mimic different possible environmental scenarios (e.g. pH, salinity, presence of proteins, etc.) occurring at the intestinal lumen, thus allowing the study of NP interactions with the media components and, once internalized, with the intracellular environment. In a recently study, it was shown that AgNP bioavailability and toxicity in the intestine is linked to the composition of its luminal content[11]. Although the RTgutGC cell culture system represents a less complex model in comparison to the intact fish intestine, it offers advantages in comparison to in vivo models such as easier manipulations of the luminal medium. Also, in comparison to ex vivo models (i.e. gut sac) it offers an easier high-throughput approach and allows longer exposure times (Minghetti et al., 2017 Cell Biol Toxicol). The RTgutGC cell system is also more ethical reducing the burden on animal testing.

The agglomeration and dissolution of MeNPs and the speciation of the resulting aqueous metals in the exposure media can be determined in simplified media of known composition[11,20]

(Figure 1). Speciation of metal in a simplified exposure medium can be achieved by using chemical equilibrium models. However, determination of intracellular MeNPs' transformations and the speciation of the metal ions released from the NP surface is challenging. It was shown recently that by feeding relevant stability constants into chemical equilibrium models allows the simulation of intracellular chelation reactions[21]. However, chemical equilibrium models are not comprehensively parameterized for the complex intracellular environment and are not designed to predict the transformations that metal nanoparticles can undergo in such environment. Electron microscopy and Raman spectroscopy techniques are sensitive to MeNPs but cannot detect dissolved or biomolecule-bond metals. In contrast, X-ray absorption spectroscopy (XAS) is optimally suited for the non-destructive determination of the speciation of metals *in situ*, even at low concentrations, or when metal occurs as diffuse dissolved or complexed species rather than concentrated particles[22]. Therefore, the use of chemical equilibrium models in conjunction with *in situ* XAS measurements allows to study the link between extracellular metal speciation with intracellular metal speciation. In this study, RTgutGC cells were cultured on transwells allowing the formation of a polarized epithelium[19] to simultaneously track intracellular silver accumulation, speciation and bioreactivity following exposure to silver nitrate and silver nanoparticles.

2. Experimental

2.1 RTgutGC cell culture

RTgutGC were kindly gifted by Kristin Schirmer (Eawag, CH). Preparation of the polarized RTgutGC epithelium was performed exactly as described priviosly[19]. Briefly, RTgutGC cells were seeded at 62,500 cells/cm^2, counting cells with the Countess II^{TM} Automated Cell Counter (Thermofisher, Waltham, MA, USA) onto transparent tissue culture inserts for multiwell plates (pore size = 0.4 µm; polyethylene terephthalate [PET] from Greiner Bio-One, Monroe, NC, USA). Insert size was chosen depending on the application (see the following): 0.33 cm^2 inserts

(for 24-well plates) for cell viability, and 4.52 cm^2 inserts (for 6-well plates) for quantitative PCR (qPCR), silver quantification by ICP-MS and XAS analysis. RTgutGC cell were culture in symmetrical conditions (i.e., with identical medium in the apical and basolateral chamber) in in Leibovitz's L-15 medium without phenol red (Thermofisher, Waltham, MA, USA) supplemented with 5% foetal bovine serum (FBS, Cat. No. F2442, Sigma-Aldrich, St. Louis, MO, USA) and 1% gentamicin (10 mg/mL, Gibco, Thermofisher, Waltham, MA, USA). The medium was changed weekly and trans epithelial electrical resistance (TEER) was monitored before medium change using an epithelial tissue voltohmeter (EVOM2; World Precision Instruments, USA) fitted with chopstick electrodes (STX-2). In all cases TEER reached 30 ohms* cm^2 by 21 days. All experiments were performed on RTgutGC cells cultured on inserts for 21 days.

2.2 Exposures

All exposures were performed as previously described[11]. Citrate coated silver NP were purchased as aqueous suspension with a concentration of total silver of 1 g/L (9.27mM, pH = 6.46). Experimental solutions were prepared freshly in the exposure medium L-15/ex[11]. L-15/ex has identical salts and sugars composition to the commercial cell culture media Leibovitz's L-15 (Gibco/ Thermofisher, Waltham, MA, USA) but does not contain amino acids and vitamins. L-15/ex pH is 7.4 Silver nitrate (Sigma-Aldrich, St. Louis, MO, USA) stock solution was prepared at a concentration of 10 mM in nanopure water (16–18 $M\Omega cm^{-1}$ Barnstead GenPure Water, Thermofisher, Waltham, MA, USA) and diluted right before each experiment in L-15/ex. Silver nitrate and cit-AgNP stock solutions were prepared to contain identical nominal concentrations of total silver. The citrate coated silver nanoparticles (cit-AgNP, nominal size: 19 nm, NanoSys GMbH, Wolfhalden, Switzerland) characterization in the exposure medium L-15/ex is reported in Figure 2. The nanoparticle agglomerate (Z-average) size and zeta potential of cit-AgNP were measured by dynamic light scattering (DLS) and electrophoretic mobility using a Zetasizer (Nano ZS, Malvern Instruments, Malvern, UK). Citrate coated AgNP dissolution was measured

by ultracentifugation as previously described [20]. Twenty-five mL of cit-AgNP suspensions were centrifuged at 145000 g (Beckman Coulter, Optima XE-90 Ultracentrifuge) for 3 h. A volume of 1 mL supernatant was digested with 0.725 mL of 69% HNO_3 for 1 hour at room temperature. The digests were diluted 10-times and measured by inductively coupled plasma-mass spectrometer (ICP-MS, iCAP Qc Thermo Scientific, USA). The recovery of $AgNO_3$ in ultra- centrifugation was over 98%. The reliability of the measurements was determined using specific water references (CPI International, USA). After 21 days of culture on transwells[19], the polarized epithelium was washed twice with a phosphate buffer (PBS, Gibco, Thermofisher, Waltham, MA, USA) then cit-AgNP or $AgNO_3$ suspensions were applied at concentrations ranging from 0.1 to 54 μg/mL in L-15/ex to determine the dose-response curve. In addition, to compare the toxicity and accumulation of $AgNO_3$ and cit-AgNP cells were exposed side by side to the same concentrations of $AgNO_3$ and cit-AgNP (i.e. 5 and 10 μM) and viability and silver uptake were measured. Furthermore, three identical sets of polarized RTgutGC were exposed to non-toxic doses of $AgNO_3$ (1 μM) and cit-AgNP (10 μM or 1.08 μg/mL) for 1, 24 and 72 hours for: i) intracellular metal concentration by ICP-MS ii) messenger RNA quantification by quantitative RT-PCR and iii) intracellular metal speciation by XAS.

2.3 Assessment of cell viability

Following exposure, the polarized RTgutGC cells have been washed twice with PBS. Assessment of cell viability was performed by means of the fluorescent dyes, Alamar blue (AB; Thermofisher, Waltham, MA, USA), 5-carboxyfluorescein diacetate acetoxymethyl ester (CFDA-AM; Thermofisher, Waltham, MA, USA) and Neutral Red (NR; Sigma-Aldrich, St. Louis, MO, USA) which are indicators of cell metabolic activity, cell membrane integrity and lysosome integrity as previously described[23]. Fluorescence was recorded using a Cytation5 plate reader

(BioTek, USA) at respective excitation/emission wavelengths of 530/595 nm for AB, 485/530 nm for CFDA-AM and 530/635nm for NR.

2.4 Quantification of intracellular silver accumulation

Intracellular silver concentration was measured by ICP-MS. Following exposure, silver determination in the polarized RTgutGC cells has been performed as previously described[23]. To ensure thorough removal of loosely bond silver, the cells were washed twice with a solution of 0.5 mM cysteine in PBS. The cells were then lysed by applying 1 mL of 50 mM NaOH to the well and incubated at room temperature for 2 hours. An aliquot (100 µL) of the cells' lysate was used for protein quantification using the modified Lowry assay (Thermo Scientific, Waltham, USA). For metal determination, cell lysates were desiccated using a concentrator (Concentrator Plus, Eppendorf, Hamburg, Germany) and digested overnight by adding 0.8 mL of 69% HNO_3. Acidified solutions were then resuspended and transferred to a Teflon tube containing 0.2 mL of 30% H_2O_2 and digested further in a digestion system (PicoTrace GmbH, Bovenden, Germany) at a maximum temperature of 180°C for 30 minutes. The digest was then diluted 10 times with nanopure water and measured. The reliability of the measurement was determined using specific references (CPI International, USA). Silver concentration in cell lysates is reported as ng Ag per mg of protein determined from the same samples to take into account cell growth.

2.5 Quantification of Metallothionein mRNA levels

Metallothionein mRNA levels in RTgutGC were measured exactly as previously described[11].

2.6 Determination of intracellular silver species by X-ray absorption spectroscopy:

After exposure cells were washed twice times with Versene solution (0.48 mM EDTA in PBS, Thermo Fisher Scientific, USA) and dislodged by trypsinization (0.25% Trypsin/EDTA solution in

PBS, Gibco, Thermofisher, Waltham, MA, USA). The trypsinization reaction was stopped by re-suspending the cells in L-15 medium supplemented with 5% FBS. Afterword cells were washed by centrifugation at 500 g for 3 minutes and re-suspension in L-15/ex. Cell viability in the washed cells was checked using the trypan blue exclusion assay with the automated cell counter Countess II (Thermofisher, Waltham, MA, USA) and was always over 90%. Finally, cells were pelleted by centrifugation at 500 g for 3 minutes the supernatant was aspirated and the pellet was immediately frozen in liquid nitrogen and placed on a sample holder made of Kel-F®, sealed with Kapton tape, and stored at -80°C. This prevented cell damage, shut down cell activity, and inhibited oxidative or chemical alteration of silver during transport or data collection[24]. The samples were transported to the Advanced Photon Source (APS) frozen on dry ice in sealed sample holders.

At the APS, these holders were mounted in a Linkham THMS6000 stage cooled to 77K with liquid N_2 at beamline 5-BM-D. Fluorescence yield X-ray absorption near-edge structure (XANES) spectra (Figure 5) were collected at the Ag K-edge using a pair of 4-element Vortex energy dispersive Si-drift detectors. Eight to twelve spectra were collected for each sample and then averaged to obtain the reported data. The incident beam energy was scanned using a Si(111) double-crystal monochromator. The energy was calibrated using a Ag metal foil, with the first inflection point in the Ag K-edge set to 25.514 keV. The spectra of known Ag compounds (Figure S2) were collected in transmission or in total fluorescence yield using a PIPS detector, with samples mounted as dry powders on cellulose acetate tape. A silver-cysteine complex was prepared by modifying a procedure for Zn-cysteine complexes[25]. 84.8 mg of L-cysteine was added to 10 mL of 7 mM $AgNO_3$. The resulting acidic pH was neutralized to pH 7 with 0.27 mL 1 M NaOH. The solution was then freeze dried and the powder was mounted on tape. The spectrum of AgCl was taken from Sekine et al., (2015)[26].

While quantitative Ag contents were not determined, the relative concentration of Ag in each sample was obtained from the change in Ag K_α X-ray fluorescence intensity across the K absorption edge, i.e., the edge step[27]. The spectra were background subtracted and normalized in the Athena interface[28] to IFEFFIT[29]. Target transformation[30] using three components well reconstructed the spectra of AgCl, AgNP, Ag-cysteine, and Ag_2S. Ag-cysteine and Ag_2S have similar XANES spectra (Figure S2), with subtle difference in fine structure at the edge and in the position of oscillations above 25530 eV. Both spectra were reconstructed well except for the broad feature centered near 25570 eV, which is more intense for Ag_2S and was not fully reproduced. Given this analysis and the expression of cysteine-rich MT upon Ag exposure (Figure 4), Ag-cysteine was used in subsequent fitting of the spectra, although the current data cannot rule out the formation of Ag_2S. The spectra of AgNP and bulk metallic Ag are also visually similar (Figure S2) but the bulk metal has larger amplitude oscillations above the absorption edge, and this amplitude was not accurately reproduced via target transformation. Silver speciation in the samples was then determined using linear-combination fitting of the XANES spectra. Samples exposed to dissolved $AgNO_3$ were fitted using the spectra of AgCl and Ag-cysteine. Fitting of the spectra of samples exposed to AgNPs included these two spectral standards along with the spectrum of AgNP. All spectra were well reproduced (Figure 5) with component sums close to 1.

2.6 Data analysis

Statistical analysis was performed using GraphPad Prism Version 7.0 (GraphPad Software Inc., San Diego, CA). Fluorescent units obtained in the cell viability assays were converted to percentage viability of control cells. The non-linear regression sigmoidal dose-response curve fitting module using the Hill slope equation was used to fit the dose-response curve data. Statistical analysis for multiple groups of data was performed by the analysis of variance

(ANOVA) followed by Tukey's post hoc test. When comparing to a control group, Dunnett's test was applied after the ANOVA. Values of $p<0.05$ were considered statistically significant.

3 Results and Discussion

3.1 Citrate coated AgNP characterization in exposure medium

Citrate coated AgNP at 10 μM show a size distribution of 84 ± 7 nm immediately after preparing the solution in L-15/ex (i.e. time 0) and agglomerate rapidly reaching 795 ± 33 nm in size with a z-potential of about -18 mV within 24 hours, after which agglomerate size remains stable for at least 72 hours (Figure 2). Citrate coated AgNP dissolution in L-15/ex is about 6% as determined by ultracentrifugation (Figure 2). The characterization of the same cit-AgNP in L-15/ex is in line with previous studies[11,20].

3.2 Cell viability studies

Previous *in vitro* studies looking at the intracellular toxicity and chemical transformations of AgNP focused on mammalian *in vitro* models where cells were exposed in complete medium containing 5-10% FBS[31–34], therefore mimicking the exposure of cells to bloodborne silver. In the blood AgNP or silver salts would reach the cells typically complexed to proteins and/or amino acids. The uptake process and intracellular transformation of silver and silver nanoparticle in absence of proteins or amino acids i.e., in polarized fish gut cells might be different from that of non-polarized mammalian cells exposed in presence of FBS. Importantly, aminoacidic complexation lowers toxicity most likely due to complexation of dissolved silver from the AgNP surface by amino acids and proteins[11]. For instance, it was previously shown that the presence of amino acids ameliorates significantly silver nitrate and cit-AgNP toxicity due to complexation of silver ions with cysteine[11,35]. For cell types which are normally surrounded by the blood, such an exposure scenario is relevant because it represents the route of exposure *in vivo.* However,

for studies using a polarized intestinal epithelium it is also relevant to study exposures with and without amino acids and protein which is physiologically relevant[23,36]. In this study, silver nitrate and cit-AgNP were dissolved or dispersed in the exposure medium L-15/ex[11] which does not contain amino acids. In L-15/ex, dissolved silver is mostly present as negatively charged silver chloride complex ($AgCl_2^-$) (Figure S1). The cell viability studies showed that silver nitrate is more toxic than cit-AgNP after 24 hours of exposure in RTgutGC polarized cells (Figure 3). Indeed, equimolar amounts of cell associated silver (Figure 3C) resulted in a different toxicity response in RTgutGC (Figure 3B). Moreover, as shown previously[11,20,23], the multiple endpoint assay indicated that lysosomes are the target of cit-AgNP whereas $AgNO_3$ affects more cell metabolic activity (Figure 3B).

For the silver uptake, silver speciation and MT mRNA quantification cells were exposed to non-toxic doses of silver nitrate and cit-AgNP (Figure 3A) for 1, 24 and 72 hours. In a previous study, it was shown that cit-AgNP toxicity in RTgutGC reached a maximum at 24 hours and then remained constant until 72 hours[11]. Therefore, the highest non-toxic exposure concentrations (1 μM $AgNO_3$ or 10 μM equivalent of cit-AgNP; Figure 3A) were applied to polarized RTgutGC to allow quantification of intracellular silver by ICP-MS and detection of intracellular silver species by XAS but without compromising the overall cell health.

3.3 $AgNO_3$ and cit-AgNP uptake over time

Silver accumulated in RTgutGC cells in a linear and time dependent manner (Figure 4A). Moreover, RTgutGC cells exposed to 10 μM equivalent of cit-AgNP accumulated a maximum of 3.7-fold more silver in comparison to cells exposed to 1 μM $AgNO_3$, which suggests that the latter is more bioavailable. However, the accumulation of cit-AgNP was faster in cells as shown by the higher slope of the intracellular silver vs time linear relationship (figure 4A and SI). The faster accumulation could be explained by the nanoparticle agglomeration behavior in L-15/ex

medium which might result in an incremental precipitation over time (Figure 2). Silver accumulation in RTgutGC could also be deduced by the florescence counts per seconds (Table S1). Although this quantification can only be considered as semi-quantitative the florescence counts gave a comparable silver accumulation over time, especially in cells exposed to cit-AgNP.

3.4 Intracellular silver speciation and MT mRNA abundance after exposure to $AgNO_3$ or cit-AgNP over time

Analysis of the X-ray absorption near-edge structure (XANES) region of XAS data (Figure 5) indicated that intracellular silver speciation changed over time in both exposure series (Figure 6). Principal component analysis on the six sample spectra required three components to reconstruct all data adequately, suggesting that three species are present in the sample set. At the earliest time point (1 hour) intracellular silver speciation is dominated by chloride complexation in both exposures. After one hour of exposure, cells exposed to $AgNO_3$ showed ~90% of Ag present as AgCl species and ~10% as Ag-cysteine complex. Cells exposed to cit-AgNP showed 78% of Ag present as AgCl and 18% as Ag^0-NP. The presence of Ag complexed to cysteine is uncertain as the abundance of this species was within error of zero. Although the cells were washed twice with Versene (0.48 mM EDTA in PBS) to remove loosely bond metal, we cannot exclude that some silver could be adsorbed on the cells and not necessarily be internalized. Alternately the silver chloride complexes could enter the cells via: i) passive diffusion if neutral complexes are formed[9] or ii) AgCl could be reduced at the cell membrane, silver could then enter as a free ion via copper transporters (e.g., CTR1[13,37,38]) and then readily re-complex with chloride, which is abundant in the cell cytoplasm. Intracellular silver chloride complexation has previously been reported in neuronal cell lines after 24 hours of exposure to AgNP (10-30% of total silver species[33]) and in a hepatic cell line exposed for 6 and 24 hours (2-4% of total silver species[39]). In our study, the percentage of detected silver chloride is higher.

This could be explained by the extracellular silver speciation (Figure S1). In L-15/ex silver chloride is the dominant species whereas in the mammalian studies mentioned above, exposures were performed in media containing amino acid and FBS, which would readily complex with dissolved silver thus reducing the extracellular silver chloride concentration. Moreover, these data suggest that, at early time points, i.e. after one hour of exposure, most silver is adsorbed on the cell membrane or is internalized as dissolved silver chloride. Silver chloride complexation dominates also in cells exposed to $AgNO_3$ for 24 hours and then shifts to being complexed by cysteine, or possibly as Ag_2S (Figure S2), in cells exposed for 72 hours. Although formation of Ag_2S inert precipitates have been previously shown in individual exposed chronically to silver[40], complexation with cysteine fit better our results due to the massive induction of the cysteine rich protein, MT mRNA at 24 hours, and, to a smaller extent at 72 hours of exposure (Figure 4B). Obtaining XAS spectra into the extended X-ray absorption fine structure (EXAFS) region, was not possible in the present study because of the noise level in the data, and imaging via transmission electron microscopy coupled with energy-dispersive spectrometry is needed to unambiguously distinguish the presence of silver cysteine complexes from Ag_2S precipitates in RTgutGC.

The silver uptake data in combination with the XAS data suggests that cit-AgNP uptake is gradual (Figure 4A, 6 and Table S1). Initially, i.e., after one hour of exposure, dissolved silver chloride species were the most abundant species entering or adsorbing to the cell while cit-AgNP uptake required more time. After 24 hours and 72 hours, cit-AgNP is internalized by endocytosis and accumulates into the lysosomes as shown by the reduced lysosome membrane integrity in the viability studies (Figure 3B and[11,23]). After 24 and 72 hours of exposure over >90% of intracellular silver is present as Ag^0-NP and the remaining silver is present as a complex with cysteine. Therefore, these data show that internalized cit-AgNP stay mainly as reduced Ag^0-NP for up to 72 hours in RTgutGC cells. About 5-7% of silver might dissolve from the cit-AgNP surface and complex readily with the thiol group of MT, which is also

highly induced by cit-AgNP (Figure 4B). It should be noted that in L-15/ex medium, cit-AgNP suspension shows ~7% dissolution (Figure 2) thus fitting the 5-7% of Ag-cysteine complexes. Previous studies, where mammalian cells have been exposed to AgNP for 24 hours showed 38%[31], 30-80%[33], 43%[32],61%[41], and 51-73%[39] of total accumulated silver as Ag^0-NP, which suggests that in mammalian cells a higher percentage of silver is dissolved intracellularly from the nanoparticle surface compared to the fish intestinal cells. The second most important silver species in common with other mammalian studies and our fish cells study is Ag-S- (most likely Ag complexed with the thiol group in glutathione or metallothionein) which was detected at 61%[31], 20-50%[33], 33%[32], 39%[41], and 21-46%[39]. In addition, Ag-O- was detected at 26%[32], 10-20%[33] and 2%[39] and AgCl at 10-30%[33] and 3-4%[39]. A couple of considerations should be made when comparing exposures in mammalian cells and our study which used fish cells: i) mammalian cells are cultured at 37ºC whereas fish cells are cultured at 19ºC which results in a higher cell metabolism[42]; ii) the mammalian studies have used concentrations 10 times higher than our study which might have resulted in a higher intercellular stress response. As mentioned earlier, the doses of $AgNO_3$ and cit-AgNP were not toxic, suggesting that at this concentration, MT is able to scavenge most dissolved silver in the cell. Remarkably, in cells exposed to $AgNO_3$ and cit-AgNP for 72 hours MT mRNA levels drop significantly in comparison to levels shown in cells exposed for 24 hours while silver concentration increases. This can be explained by the fact that almost all dissolved Ag is complexed to cysteine which detoxifies silver and inhibits the induction of MT mRNA levels, an effect previously shown in RTgutGC cells exposed to cit-AgNP[11].

Conclusions

This study shows how analysis of extracellular and intracellular metal speciation can clarify the intracellular chemical fate of metals and metal nanoparticles. Moreover, this approach brings a new insight to our understanding of Ag and cit-AgNP uptake and bio-reactivity in fish intestinal

cells. One major aspect of this study is that while most aquatic toxicology literature indicates that fish can readily take up Ag^+ but not AgCl complexes, our data show that the intestinal cell RTgutGC can take up (or adsorb) silver as AgCl complexes, which are subsequently bioavailable and bio-reactive.

Moreover, it was shown in *in vitro (*[23] and Figure 3C), *ex vivo*[36] *and in vivo*[43] studies that the intestinal epithelium accumulates similar concentrations of silver when exposed to equimolar amounts of $AgNO_3$ or AgNP. However, at least in *in vitro* studies cit-AgNP is about 10-15 times less toxic than $AgNO_3$[11,20,44]. In this study, we demonstrate that at equimolar amounts of intracellular silver concentrations $AgNO_3$ is more toxic than cit-AgNP, at least after acute exposures (i.e. 24 hours). The intracellular silver speciation therefore supports the hypothesis that dissolved silver species are more toxic than zero-valent silver nanoparticles. Overall, our data supports previous *in vivo*[43] and *in vitro*[23] studies where silver nanoparticles present a similar but attenuated toxic response to ionic silver ($AgNO_3$). Thus, at least in acute exposures, existing risk assessment for dissolved silver species would also be protective for nano-silver. However, under chronic exposure scenarios an increase in silver nanoparticle toxicity cannot be excluded due to a potential increase in intracellular silver dissolution.

Conflicts of interest

There are no conflicts to declare

Acknowledgements

This research was supported by the U.S. National Science Foundation (NSF) Biological and Environmental Interactions of Nanoscale Materials program through award nos. CBET-1706093 (M.M.) and CBET-1704362 (J.G.C.). The XAS measurements were performed at the DuPont-Northwestern-Dow Collaborative Access Team (DND-CAT) located at Sector 5 of the Advanced Photon Source (APS). DND-CAT is supported by Northwestern University, E.I. DuPont de

Nemours & Co., and The Dow Chemical Company. This research used resources of the Advanced Photon Source, a U.S. Department of Energy (DOE) Office of Science User Facility operated for the DOE Office of Science by Argonne National Laboratory under Contract No. DE-AC02-06CH11357. The authors wish to thank Professor Kristin Schirmer (eawag, CH) for providing the cell line RTgutGC used in this study.

References

1 EU, *Off. J. Eur. Union*, 2011, **275**, 38–40.
2 R. Behra, L. Sigg, M. J. D. Clift, F. Herzog, M. Minghetti, B. Johnston, A. Petri-Fink, B. Rothen-Rutishauser and B. Rothen-Rutishauser, *J. R. Soc. Interface*, 2013, **10**, 20130396.
3 J. R. Morones-Ramirez, J. A. Winkler, C. S. Spina and J. J. Collins, *Sci. Transl. Med.* , 2013, **5**, 190ra81-190ra81.
4 E. K. Hill and J. Li, *J. Anim. Sci. Biotechnol.*, 2017, **8**, 1–13.
5 P. Swain, S. K. Nayak, A. Sasmal, T. Behera, S. K. Barik, S. K. Swain, S. S. Mishra, A. K. Sen, J. K. Das and P. Jayasankar, *World J. Microbiol. Biotechnol.*, 2014, **30**, 2491–2502.
6 P. R. Paquin, J. W. Gorsuch, S. Apte, G. E. Batley, K. C. Bowles, P. G. C. Campbell, C. G. Delos, D. M. Di Toro, R. L. Dwyer, F. Galvez, R. W. Gensemer, G. G. Goss, C. Hogstrand, C. R. Janssen, J. C. McGeer, R. B. Naddy, R. C. Playle, R. C. Santore, U. Schneider, W. A. Stubblefield, C. M. Wood and K. B. Wu, *Comp. Biochem. Physiol. Part C Toxicol. Pharmacol.*, 2002, **133**, 3–35.
7 J. Genz, A. J. Esbaugh and M. Grosell, *Comp. Biochem. Physiol. A. Mol. Integr. Physiol.*, 2011, **159**, 150–8.
8 E. A. Ferguson and C. Hogstrand, *Environ. Toxicol. Chem.*, 1998, **17**, 589–593.
9 N. R. Bury and C. Hogstrand, *Environ. Sci. Technol.*, 2002, **36**, 2884–8.
10 C. M. Zhao, P. G. C. Campbell and K. J. Wilkinson, *Environ. Chem.*, 2016, **13**, 425–433.
11 M. Minghetti and K. Schirmer, *Nanotoxicology*, 2016, **10**, 1526–1534.
12 E. J. Martinez-Finley, S. Chakraborty, S. J. B. Fretham and M. Aschner, *Metallomics*, 2012, **4**, 593–605.
13 M. Minghetti, M. J. Leaver, E. Carpenè and S. G. George, *Comp. Biochem. Physiol. Part C Toxicol. Pharmacol.*, 2008, **147**, 450–459.
14 M. Minghetti, M. J. Leaver and S. G. George, *Aquat. Toxicol.*, 2010, **97**, 23–33.
15 M. I. Setyawati, X. Yuan, J. Xie and D. T. Leong, *Biomaterials*, 2014, **35**, 6707–15.
16 C. Levard, E. M. Hotze, B. P. Colman, A. L. Dale, L. Truong, X. Y. Yang, A. J. Bone, G. E. Brown, R. L. Tanguay, R. T. Di Giulio, E. S. Bernhardt, J. N. Meyer, M. R. Wiesner and G. V. Lowry, *Environ. Sci. Technol.*, 2013, **47**, 13440–13448.
17 M. Auffan, C. W. Matson, J. Rose, M. Arnold, O. Proux, B. Fayard, W. Liu, P. Chaurand, M. R. Wiesner, J.-Y. Bottero and R. T. Di Giulio, *Nanotoxicology*, 2014,

8, 167–176.
18 K. J. Groh, T. Dalkvist, F. Piccapietra, R. Behra, M. J.-F. Suter and K. Schirmer, *Nanotoxicology*, 2014, **5390**, 1–11.
19 M. Minghetti, C. Drieschner, N. Bramaz, H. Schug and K. Schirmer, *Cell Biol. Toxicol.*, 2017, **33**, 539–555.
20 Y. Yue, R. Behra, L. Sigg, P. Fernández Freire, S. Pillai and K. Schirmer, *Nanotoxicology*, 2015, **9**, 54–63.
21 J. A. Rees, G. J. P. Deblonde, D. D. An, C. Ansoborlo, S. S. Gauny and R. J. Abergel, *Sci. Rep.*, 2018, **8**, 2–10.
22 R. Ortega, *J. Anal. At. Spectrom.*, 2011, **26**, 23–29.
23 M. Minghetti and K. Schirmer, *Environ. Sci. Nano*, 2019, **6**, 1777.
24 S. Roudeau, A. Carmona, L. Perrin and R. Ortega, *Anal. Bioanal. Chem.*, 2014, **406**, 6979–6991.
25 S. Beauchemin, D. Hesterberg, J. Nadeau and J. C. McGeer, *Environ. Sci. Technol.*, 2004, **38**, 1288–1295.
26 R. Sekine, G. Brunetti, E. Donner, M. Khaksar, K. Vasilev, A. K. Jämting, K. G. Scheckel, P. Kappen, H. Zhang and E. Lombi, *Environ. Sci. Technol.*, 2015, **49**, 897–905.
27 S. D. Kelly, D. Hestberg and B. Ravel, in *Methods of Soil Analysis, Part 5 - Mineralogical Methods*, Soil Science Society of America, Madison, WI, 2008, pp. 367–463.
28 B. Ravel and M. Newville, *J. Synchrotron Radiat.*, 2005, **12**, 537–541.
29 M. Newville, *J. Synchrotron Radiat.*, 2001, **8**, 322–324.
30 A. Manceau, M. A. Marcus and N. Tamura, *Rev. Mineral. Geochemestry*, 2002, **49**, 341–428.
31 X. Jiang, T. Miclăuş, L. Wang, R. Foldbjerg, D. S. Sutherland, H. Autrup, C. Chen and C. Beer, *Nanotoxicology*, 2015, **9**, 181–189.
32 L. Wang, T. Zhang, P. Li, W. Huang, J. Tang, P. Wang, J. Liu, Q. Yuan, R. Bai, B. Li, K. Zhang, Y. Zhao and C. Chen, *ACS Nano*, 2015, **9**, 6532–6547.
33 I.-L. Hsiao, Y.-K. Hsieh, C.-F. Wang, I.-C. Chen and Y.-J. Huang, *Enviromental Sci. Technol.*, 2015, **49**, 3813–21.
34 Y.-H. Lee, F.-Y. Cheng, H.-W. Chiu, J.-C. Tsai, C.-Y. Fang, C.-W. Chen and Y.-J. Wang, *Biomaterials*, 2014, **35**, 4706–15.
35 E. Navarro, F. Piccapietra, B. Wagner, B. Wagner, F. Marconi, F. Marconi, R. Kaegi, R. Kaegi, N. Odzak and N. Odzak, *Environ. Sci. Technol.*, 2008, 8959–8964.
36 N. J. Clark, D. Boyle and R. D. Handy, *Environ. Sci. Nano*, 2019, **6**, 646–660.
37 Y. Nose, B.-E. E. Kim and D. J. Thiele, *Cell Metab.*, 2006, **4**, 235–244.
38 J. Bertinato, L. Cheung, R. Hoque and L. J. Plouffe, *J. Trace Elem. Med. Biol.*, 2010, **24**, 178–184.
39 G. Veronesi, A. Deniaud, T. Gallon, P.-H. Jouneau, J. Villanova, P. Delangle, M. Carrière, I. Kieffer, P. Charbonnier, E. Mintz and I. Michaud-Soret, *Nanoscale*, 2016, **8**, 17012–17021.
40 A. B. G. Lansdown, *Adv. Pharmacol. Sci.*, 2010, **2010**, 1–16.
41 G. Veronesi, C. Aude-Garcia, I. Kieffer, T. Gallon, P. Delangle, N. Herlin-Boime, T. Rabilloud and M. Carrière, *Nanoscale*, 2015, **7**, 7323–7330.

42 P. Ducommun, P. A. Ruffieux, A. Kadouri, U. Von Stockar and I. W. Marison, *Biotechnol. Bioeng.*, 2002, **77**, 838–842.
43 N. J. Clark, D. Boyle, B. P. Eynon and R. D. Handy, *Environ. Sci. Nano*, , DOI:10.1039/C9EN00261H.
44 M. Connolly, M.-L. Fernandez-Cruz, A. Quesada-Garcia, L. Alte, H. Segner and J. M. Navas, *Int. J. Environ. Res. Public Health*, 2015, **12**, 5386–405.

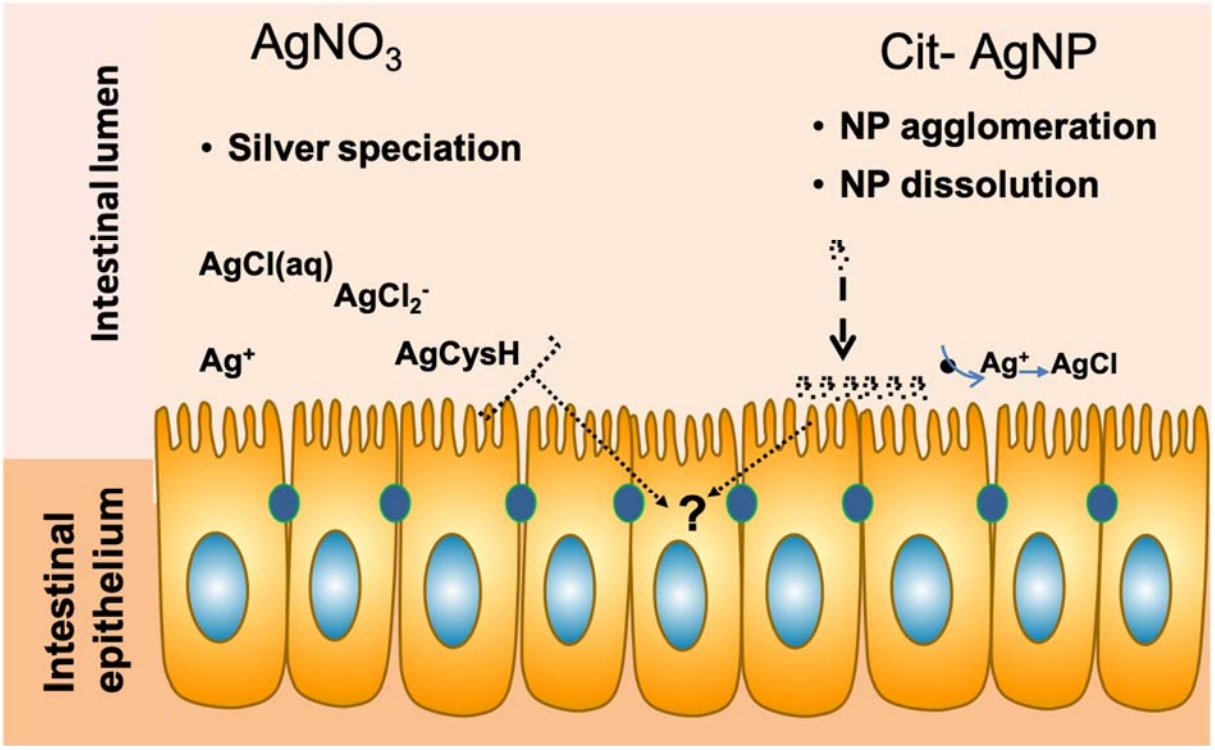

Figure 1: Conceptual representation of the measurable chemical transformations of dissolved silver and cit-AgNP in the intestinal lumen. Such transformations influence intracellular metal uptake, speciation and bio-reactivity. Analysis of dissolved silver and cit-AgNP transformations in extracellular medium include metal speciation (Visual MINTEQ), NP agglomeration (Dynamic Light Scattering) and NP dissolution (ultracentrifugation and ultrafiltration)[11,20]. Intracellular transformations can be determined by X-ray absorption spectroscopy.

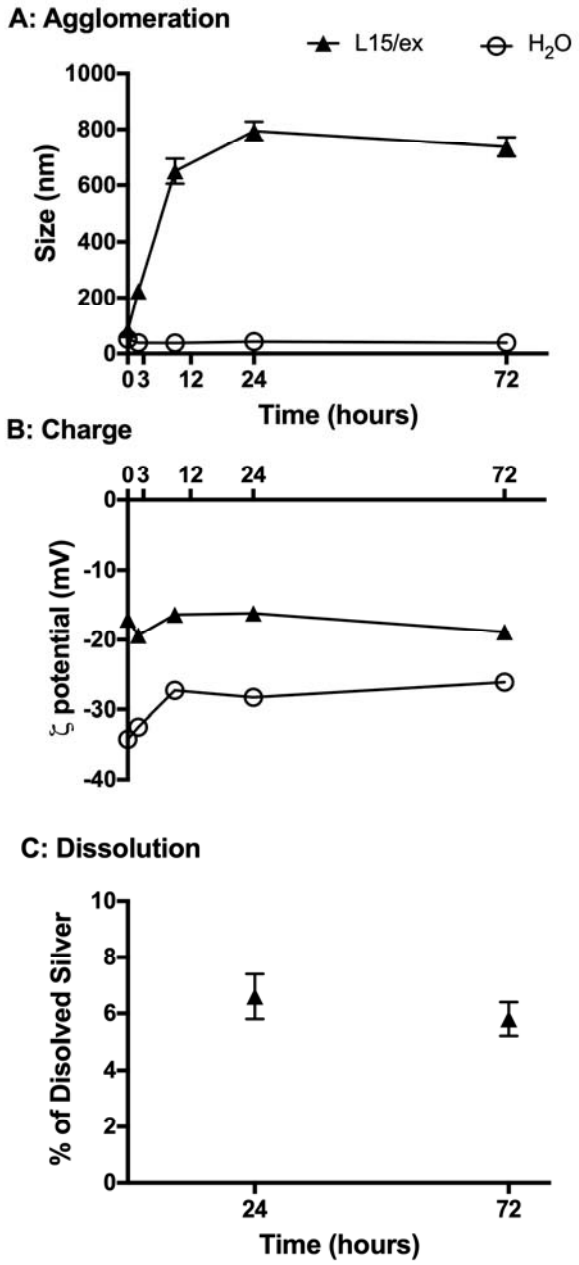

Figure 2: Cit-AgNP characterization. Size and ζ-potential of 10 μM cit-AgNP in L15-ex and water over 72 hours is reported in panel A and B, respectively. Dissolution in L-15/ex is reported in panel C. The cit-AgNP size (Z-average) and ζ potential of cit-AgNP suspensions were measured in triplicate by DLS and dissolution by ultracentrifugation. Values are mean ± SD, n=3.

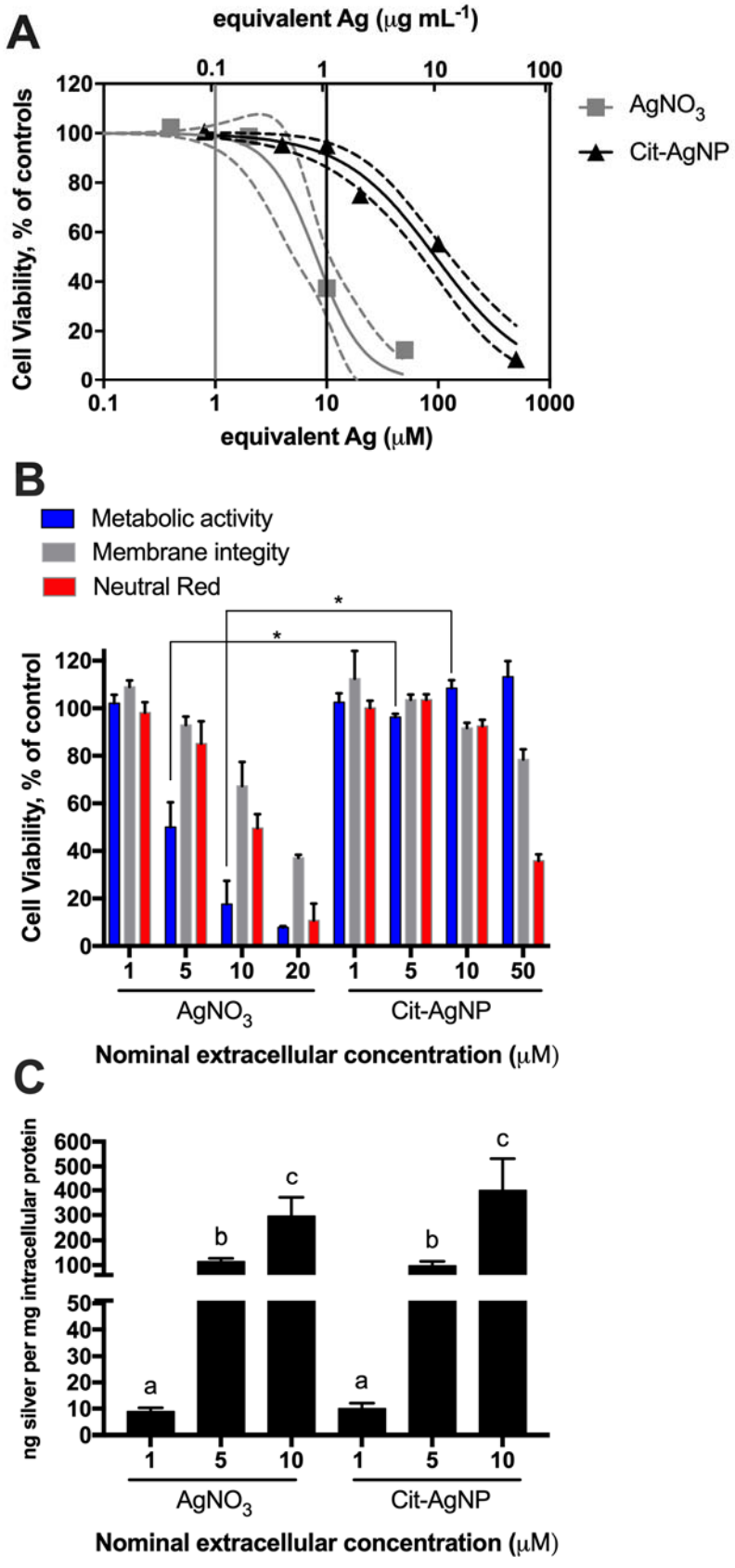
A
equivalent Ag (μg mL-1)
0.1
1
10
100
Cell Viability, % of controls
AgNO3
Cit-AgNP
equivalent Ag (μM)
B
Metabolic activity
Membrane integity
Neutral Red
Cell Viability, % of control
AgNO3
Cit-AgNP
Nominal extracellular concentration (μM)
C
ng silver per mg intracellular protein
AgNO3
Cit-AgNP
Nominal extracellular concentration (μM)

Figure 3: Toxicity of $AgNO_3$ and cit-AgNP as function of total silver in the exposure medium (L-15/ex). The endpoints measured, cell metabolic activity, cell membrane integrity and lysosome integrity, were taken after 24 hours of exposure. A, $AgNO_3$ and cit-AgNP dose-response curve using the cell membrane integrity endpoint (CFDA-AM). Values shown are averages and confidence intervals (dashed lines) of three independent experiments (n=3). Exposure concentrations of $AgNO_3$ (1 μM or 0.108 μg/mL) and cit-AgNP (10 μM or 1.08 μg/mL) are indicated by a vertical line. A double scale of equivalent silver is shown for comparison. B, multiple endpoint viability assay in RTgutGC cells exposed for 24 hours, values shown are a means ± SD (n=3). Differences in metabolic activity in cells exposed to equimolar concentrations of $AgNO_3$ and cit-AgNP (i.e. 1, 5 and 10 μM) are indicated by an asterix (1-way, $p<0.05$, 1-way ANOVA, Tukey's test). C, silver concentration determined by ICP-MS in RTgutGC cells exposed for 24 hours. Cellular-associated silver was normalized to protein content to consider possible variation in cell numbers. Values are means ± SD, n=4. Bars bearing different lettering are significantly different ($p < 0.05$, 1-way ANOVA, Tukey's test).

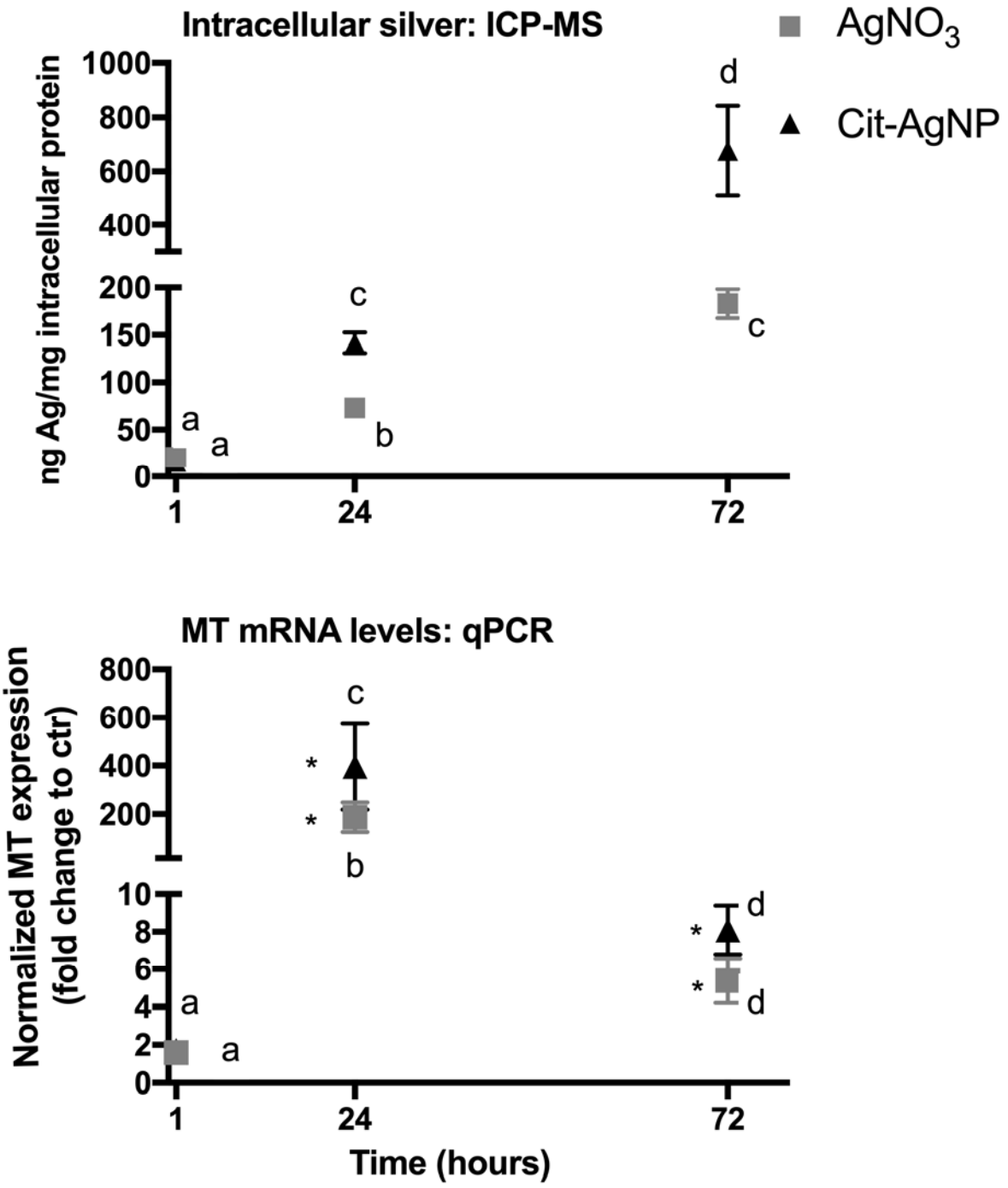

Figure 4: Intracellular silver uptake and bio-reactivity in RTgutGC exposed to non-toxic doses of $AgNO_3$ (1 μM or 0.108 μg/mL) and cit-AgNP (10 μM or 1.08 μg/mL) over 72 hours. A: Total silver determination by ICP-MS. Metal concentration in cell lysates is reported as ng silver per

mg of protein determined from the same samples to take into account differences in cell numbers. Values represent mean ± SD, n=3. Symbols bearing different lettering are statistically different ($p<0.05$, 2-way ANOVA, Tukey's test). B: Normalized mRNA levels of Metallothionein (MT). Values are expressed as ratio of the expression in those cells exposed to control media (see Figure S3). Values represent mean normalized fold change ± SD, n=3. Symbols bearing different lettering are statistically different ($p<0.05$, 2-way ANOVA, Tukey's test). Statistical difference from respective control, i.e., untreated cells at each time point is indicated by an asterisk (t-test, $p< 0.05$).

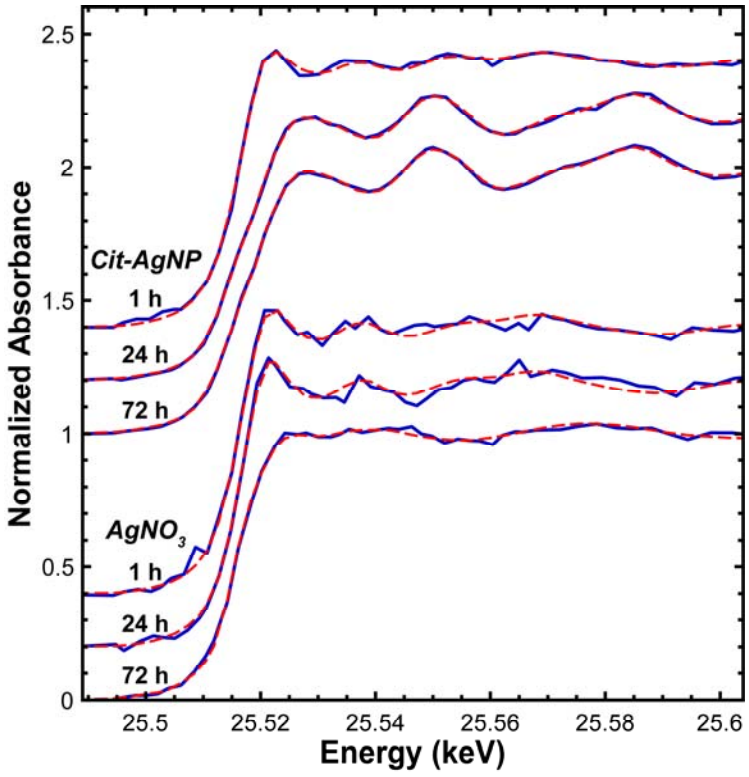

Figure 5: Ag K-edge XANES spectra of pelleted RTgutGC cells exposed to either silver nanoparticles (Cit-AgNP) or silver nitrate solution ($AgNO_3$). The data (solid blue) were fitted (dashed red) as a linear combination of the spectra of Ag chloride, Ag cysteine, or Ag nanoparticles (see Figure 5). Fitting procedures, statistical assessment of spectral variability

and appropriate fitting standards, and detailed fitting results are reported in the Supplementary Information.

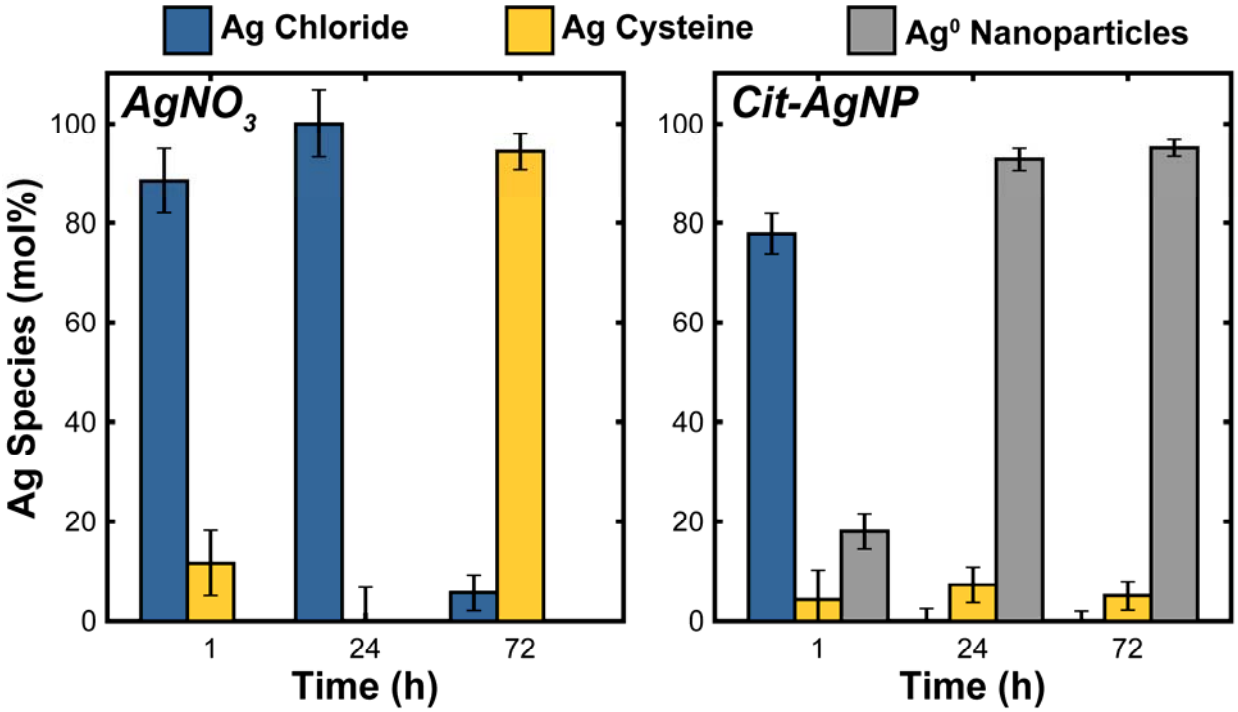

Figure 6: Intracellular silver speciation determined by linear combination fitting of the XANES spectra reported in Figure 4. Values are the molar percentages of the total Ag species in the samples, with the error bar indicating the uncertainties derived from the linear-combination fitting procedure, reported at the 1σ level (68% confidence interval).

Supplementary information:

Linking Chemical Transformations of Silver Nanoparticles in the Extracellular and Intracellular Environment to their Bioavailability and Toxicity.

Matteo Minghetti[a], Qing Ma,[b] and Jeffrey G. Catalano[c]

[a.] Department of Integrative Biology, Oklahoma State University, Stillwater, OK, USA.
[b.] DND-CAT, Northwestern Synchrotron Research Center at Advanced Photon Source, Argonne, IL, USA.
[c.] Department of Earth and Planetary Sciences, Washington University, Saint Louis, MO, USA.

Corresponding author: matteo.minghetti@okstate.edu

METHODS

RTgutGC cell culture: RTgutGC were kindly gifted by Kristin Schirmer (Eawag, CH). Preparation of the polarized RTgutGC epithelium was performed exactly as described priviosly[1]. Briefly, RTgutGC cells were seeded at 62,500 cells/cm^2, counting cells with the Countess II™ Automated Cell Counter (Thermofisher, Waltham, MA, USA) onto transparent tissue culture inserts for multiwell plates (pore size = 0.4 µm; polyethylene terephthalate [PET] from Greiner Bio-One, Monroe, NC, USA). Insert size was chosen depending on the application (see the following): 0.33 cm^2 inserts (for 24-well plates) for cell viability, and 4.52 cm^2 inserts (for 6-well plates) for quantitative PCR (qPCR), silver quantification by ICP-MS and XAS analysis. RTgutGC cell were culture in symmetrical conditions (i.e. with identical medium in the apical and basolateral chamber) in in Leibovitz's L-15 medium without phenol red (Thermofisher, Waltham, MA, USA) supplemented with 5% foetal bovine serum (FBS, Cat. No. F2442, Sigma-Aldrich, St. Louis, MO, USA) and 1% gentamicin (10 mg/mL, Gibco, Thermofisher, Waltham, MA, USA). The medium was changed weekly and trans epithelial electrical resistance (TEER) was monitored before medium change using an epithelial tissue voltohmeter (EVOM2; World Precision Instruments, USA) fitted with chopstick electrodes (STX-2). I all cases TEER reached

30 ohms* cm^2 by 21 days. All experiments were performed on RTgutGC cells cultured on inserts for 21 days.

Exposures: All exposures were performed as previously described[2]. Briefly, $AgNO_3$ and cit-AgNP stock solutions were prepared to contain identical nominal concentrations of total silver. The citrate coated silver nanoparticles (cit-AgNP, nominal size: 19 nm, NanoSys GMbH, Wolfhalden, Switzerland) characterization in the exposure medium L-15/ex has been previously reported[2,3]. Citrate coated silver NP were purchased as aqueous suspension with a concentration of total silver of 1 g/L (9.27mM, pH = 6.46). Experimental solutions were prepared freshly in the exposure medium L-15/ex[2]. Silver nitrate (Sigma-Aldrich, St. Louis, MO, USA) stock solution was prepared at a concentration of 10 mM in nanopure water (16–18 $M\Omega cm^{-1}$ Barnstead GenPure Water, Thermofisher, Waltham, MA, USA) and diluted right before each experiment in L-15/ex. After 21 days of culture on transwells[1], the polarized epithelium was washed twice with a phosphate buffer (PBS, Gibco, Thermofisher, Waltham, MA, USA). Cells were then exposed to non-toxic doses of $AgNO_3$ (1 μM) and cit-AgNP (10 μM or 1.08 μg/mL) for 1, 24 and 72 hours.

Assessment of cell viability: Following exposure, the polarized RTgutGC cells have been washed twice with PBS. Non-invasive assessment of cell viability was performed by means of the fluorescent dye, 5-carboxyfluorescein diacetate acetoxymethyl ester (CFDA-AM; Thermofisher, Waltham, MA, USA) which is an indicator of cell membrane integrity, essentially as described by Minghetti and Schirmer (2016). Florescence was recorded using a Cytation5 plate reader (BioTek, USA) at excitation/emission wavelengths of 485/530 nm.

Quantification of intracellular silver accumulation: Intracellular silver concentrations were measured by inductively coupled plasma-mass spectrometer (ICP-MS, iCAP Qc Thermo Scientific, USA). Following exposure, silver determination from the polarized RTgutGC cells

have been performed as previously described[1]. The reliability of the measurement was determined using specific references (CPI International, USA). Silver concentration in cell lysates is reported as ng Ag per mg of protein determined from the same samples to take into account cell growth.

Quantification of Metallothionein mRNA levels: Metallothionein mRNA levels in RTgutGC were measured exactly as described in Minghetti and Schirmer (2016).

Determination of intracellular silver species by X-ray absorption spectroscopy: After exposure cells were washed twice times with Versene solution (0.48 mM EDTA in PBS, Thermo Fisher Scientific, USA) and dislodged by trypsinization (0.25% Trypsin/EDTA solution in PBS, Gibco, Thermofisher, Waltham, MA, USA). The trypsinization reaction was stopped by re-suspending the cells in L-15 medium supplemented with 5% FBS. Afterword cells were washed by centrifugation at 500 g for 3 minutes and re-suspension in L-15/ex. Cell viability in the washed cells was checked using the trypan blue exclusion assay with the automated cell counter Countess II (Thermofisher, Waltham, MA, USA) and was always over 90%. Finally, cells were pelleted by centrifugation at 500 g for 3 minutes the supernatant was aspirated and the pellet was immediately frozen in liquid nitrogen and placed on a sample holder made of Kel-F®, sealed with Kapton tape, and stored at -80°C. This prevented cell damage, shut down cell activity, and inhibited oxidative or chemical alteration of silver during transport or data collection[4]. The samples were transported to the Advanced Photon Source (APS) frozen on dry ice in sealed sample holders.

At the APS, these holders were mounted in a Linkham THMS6000 stage cooled to 77K with liquid N_2 at beamline 5-BM-D. Fluorescence yield X-ray absorption near-edge structure (XANES) spectra (Figure 4) were collected at the Ag K-edge using a pair of 4-element Vortex energy dispersive Si-drift detectors. Eight to twelve spectra were collected for each sample and

then averaged to obtain the reported data. The incident beam energy was scanned using a Si(111) double-crystal monochromator. The energy was calibrated using a Ag metal foil, with the first inflection point in the Ag K-edge set to 25.514 keV. The spectra of known Ag compounds (Figure S1) were collected in transmission or in total fluorescence yield using a PIPS detector, with samples mounted as dry powders on cellulose acetate tape. A silver-cysteine complex was prepared by modifying a procedure for Zn-cysteine complexes[5]. 84.8 mg of L-cysteine was added to 10 mL of 7 mM $AgNO_3$. The resulting acidic pH was neutralized to pH 7 with 0.27 mL 1 M NaOH. The solution was then freeze dried and the powder was mounted on tape. The spectrum of AgCl was taken from Sekine et al., (2015)[6].

While quantitative Ag contents were not determined, the relative concentration of Ag in each sample was obtained from the change in Ag K_α X-ray fluorescence intensity across the K absorption edge, i.e., the edge step[7]. The spectra were background subtracted and normalized in the Athena interface[8] to IFEFFIT[9]. Target transformation[10] using three components well reconstructed the spectra of AgCl, AgNP, Ag-cysteine, and Ag_2S. Ag-cysteine and Ag_2S have similar XANES spectra (Figure S1), with subtle difference in fine structure at the edge and in the position of oscillations above 25530 eV. Both spectra were reconstructed well except for the broad feature centered near 25570 eV, which is more intense for Ag_2S and was not fully reproduced. Given this analysis and the expression of cysteine-rich metallothionein upon Ag exposure (Figure 3), Ag-cysteine was used in subsequent fitting of the spectra, although the current data cannot rule out the formation of Ag_2S. The spectra of AgNP and bulk metallic Ag are also visually similar (Figure S1) but the bulk metal has larger amplitude oscillations above the absorption edge, and this amplitude was not accurately reproduced via target transformation. Silver speciation in the samples was then determined using linear-combination fitting of the XANES spectra. Samples exposed to dissolved $AgNO_3$ were fitted using the spectra of AgCl and Ag-cysteine. Fitting of the spectra of samples exposed to AgNPs included

these two spectral standards along with the spectrum of AgNP. All spectra were well reproduced (Figure 4) with component sums close to 1.

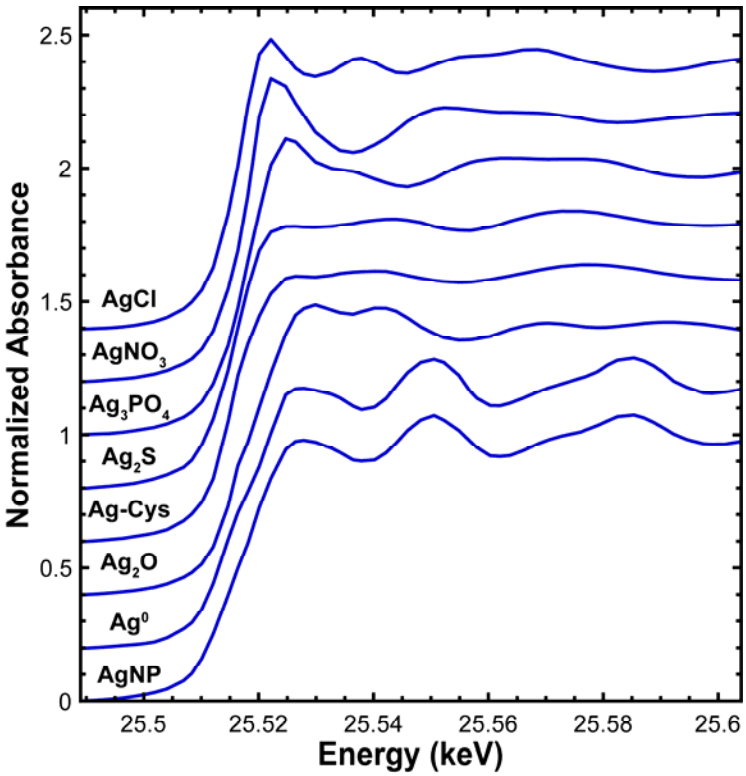

Figure S1: Ag K-edge XANES spectra of silver reference compounds; Ag-cys is silver complexed to cysteine.

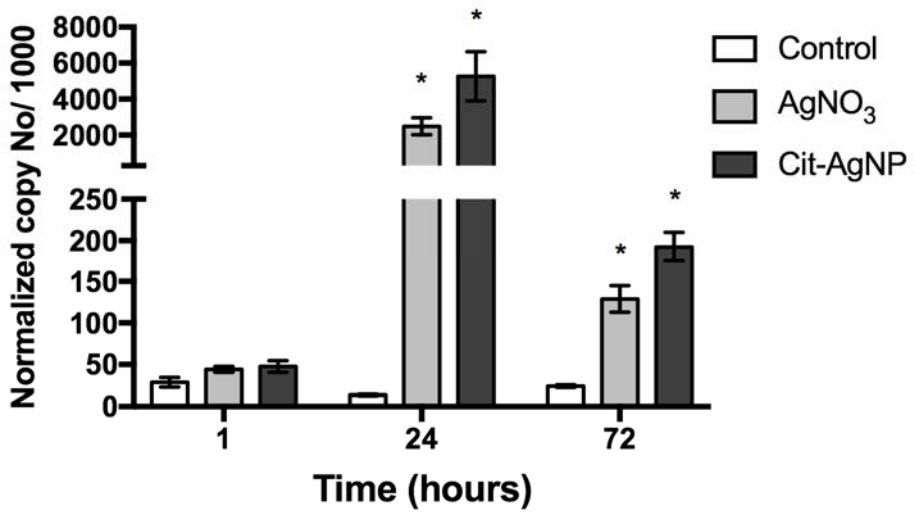

Figure S2: Normalized Metallothionein B (MTb) mRNA expression measured in RTgutGC cells exposed to 1 µM AgNO3 or 10 µM cit-AgNP in L-15/ex medium for 1, 24 and 72 hours. Values are means ± SEM (n=3). Statistical difference from respective controls for each time point is indicated by an asterisk (*)(t-test, $p < 0.05$).

Table S1. Speciation of Ag in RTgutGC determined by XANES spectroscopy.

Exposure Time	Ag K_α (cps)[a]	AgCl (mol%)	Ag-Cys (mol%)	AgNP (mol%)	Component Sum	R-factor (×10⁴)[b]	χ_v^2 (×10⁴)[b]
AgNP							
1 h	510±30[c]	78±4[d]	4±6	18±4	1.00	8.49	1.31
24 h	1050±20	0±2	7±4	93±2	1.00	3.11	0.48
72 h	2910±10	0±2	5±3	95±2	1.00	2.02	0.32
$AgNO_3$							
1 h	220±10	88±6	12±7	-	1.00	29.21	4.41
24 h	201±7	100±7	0±7	-	0.99	32.36	4.84
72 h	400±10	6±4	94±4	-	1.00	8.29	1.28

[a] Ag K_α fluorescence counts per second (cps), proportional to concentration.
[b] Goodness-of-fit parameters[7].
[c] Reported uncertainty is the standard deviation of the change in X-ray fluorescence intensity across among the individual scans that were averaged to obtain the reported data.
[d] The uncertainty in the percentage of species was determined in the linear-combination fitting procedure and are reported at the 1σ level (68% confidence interval).

References

1 M. Minghetti, C. Drieschner, N. Bramaz, H. Schug and K. Schirmer, *Cell Biol. Toxicol.*, 2017, **33**, 539–555.
2 M. Minghetti and K. Schirmer, *Nanotoxicology*, 2016, **10**, 1526–1534.
3 Y. Yue, R. Behra, L. Sigg, P. Fernández Freire, S. Pillai and K. Schirmer, *Nanotoxicology*, 2015, **9**, 54–63.
4 S. Roudeau, A. Carmona, L. Perrin and R. Ortega, *Anal. Bioanal. Chem.*, 2014, **406**, 6979–6991.
5 S. Beauchemin, D. Hesterberg, J. Nadeau and J. C. McGeer, *Environ. Sci. Technol.*, 2004, **38**, 1288–1295.
6 R. Sekine, G. Brunetti, E. Donner, M. Khaksar, K. Vasilev, A. K. Jämting, K. G. Scheckel, P. Kappen, H. Zhang and E. Lombi, *Environ. Sci. Technol.*, 2015, **49**, 897–905.
7 S. D. Kelly, D. Hestberg and B. Ravel, in *Methods of Soil Analysis, Part 5 - Mineralogical Methods*, Soil Science Society of America, Madison, WI, 2008, pp. 367–463.
8 B. Ravel and M. Newville, *J. Synchrotron Radiat.*, 2005, **12**, 537–541.
9 M. Newville, *J. Synchrotron Radiat.*, 2001, **8**, 322–324.
10 A. Manceau, M. A. Marcus and N. Tamura, *Rev. Mineral. Geochemestry*, 2002, **49**, 341–428.